BMC Medicine

RESEARCH

Open Access

Targeted long-read genomic and epigenomic profiling enhances timely comprehensive variant discovery in hypotonia and muscle weakness

Eman Abuijlan[1], Shruti Sinha[2], Sathishkumar Ramaswamy[2], Ruchi Jain[2], Ikram Chekroun[1], Fatma Rabea[1], Maha El Naofal[2], Syeda Khadija[1], Radwa Sharaf[2], Omer S. Alkhnbashi[1], Fahad Ali[1,3], Alawi Alsheikh-Ali[1,4] and Ahmad Abou Tayoun[1,2,3*]

Abstract

Background Identifying the genetic basis of hypotonia and muscle weakness is critical for patient management and family counseling. However, diagnosis is often hindered by diverse genomic alterations, including repeat expansions, structural variants (SVs), and methylation defects. Standard-of-care testing, largely based on short-read sequencing, is limited in its ability to detect this heterogeneous variation landscape, leaving many patients undiagnosed or requiring lengthy sequential testing. Long-read sequencing represents a promising solution. However, its application as a first-tier diagnostic assay for hypotonia remains unexplored.

Methods We retrospectively analyzed 227 patients with hypotonia to assess diagnostic yield, time-to-diagnosis, and costs associated with standard-of-care testing. A long-read whole-genome sequencing (LR-WGS) workflow with targeted analysis of hypotonia-associated genes was developed to detect and prioritize pathogenic SNVs, SVs, and CNVs, repeat expansions, and methylation changes at key disease loci. The workflow was validated in a reference-positive cohort with known diagnoses ($n=15$) and applied to an unsolved cohort ($n=14$). Variant interpretation followed ACMG guidelines and was confirmed with orthogonal methods.

Results Standard-of-care testing achieved a diagnostic yield of 42% with an average time-to-diagnosis of 68.7 days; however, 30% of diagnosed patients experienced significant delays (average 169 days) due to sequential testing. The LR-WGS based approach identified all known pathogenic variants in the positive cohort, including *SMN1* deletions, methylation defects at 15q11.2/Prader-Willi locus, *FMR1* repeat expansions, and sequence and copy-number variants in > 100 genes underlying myopathies and muscular dystrophies. The targeted long-read pipeline reduced prioritized variant calls by 97.9–99.9% and, in the unsolved cohort, yielded one definitive diagnosis (de novo *COL6A3* deletion) and one possible diagnosis (aberrant methylation and copy number at *POMK*), for an additional 14% yield. Among patients diagnosed after sequential testing ($n=29$), LR-WGS is expected to reduce time-to-diagnosis by ~ 85% and decrease cumulative diagnostic delays, with projected healthcare cost savings of $396,000–439,000. Across the entire 227 patient cohort, LR-WGS is anticipated to reduce testing costs by 6.5%, yielding an average savings of $105 per patient.

*Correspondence:
Ahmad Abou Tayoun
Ahmad.Tayoun@dubaihealth.ae
Full list of author information is available at the end of the article

Conclusions LR-WGS enables comprehensive discovery of genomic and epigenomic variants in hypotonia and muscle weakness, improving diagnostic yield, shortening diagnostic timelines, and reducing costs compared with current standard-of-care testing.

Keywords Hypotonia, Muscular weakness, Neuromuscular disorders, WG-LRS, SVs, CNVs, Small SNVs, STR expansion disorders, DNA methylation profiling

Background

Hypotonia, characterized by a reduction in muscle tone, can result in a loss of postural control due to decreased resistance to passive movement in the axial muscles, including those of the neck, back, trunk, as well as in the arms and legs [1, 2]. While hypotonia is not a specific diagnosis on its own, it is recognized as a key symptom in a wide range of heterogeneous rare genetic disorders, including various neuromuscular and neurodevelopmental conditions.

Clinically, hypotonia is classified into two primary types based on the neuroanatomic localization of the underlying defects: central hypotonia and peripheral hypotonia [2]. The former results from neurological dysfunction within the central nervous system (CNS) and is a prominent early, non-specific symptom in various neurodevelopmental disorders [1]. Conditions such as Prader-Willi and Angelman Syndromes (PWS/AS), which arise from imprinting defects in key genes located within an imprinted cluster on chromosome 15, as well as Fragile X Syndrome (FXS), caused by the abnormal expansion of the CGG trinucleotide repeat sequence in the 5′-untranslated region (5′UTR) of the *FMR1* gene, exemplify the diverse range of disorders associated with central hypotonia [1, 3, 4]. Conversely, peripheral hypotonia arises from lesions affecting the peripheral motor unit, which includes defects in the lower motor neurons (anterior horn cells of the spinal cord), peripheral nerves, neuromuscular junctions, and the skeletal muscles themselves [5]. Consequently, peripheral hypotonia is often considered the primary manifestation of many neuromuscular disorders, including spinal muscular atrophy (SMA), congenital myasthenic syndromes, congenital myopathies (CMs), myotonic dystrophy (DM), and various forms of muscular dystrophy (MD), such as Duchenne muscular dystrophy (DMD) [6, 7]. Each of these disorders has a distinct genetic etiology, which may involve structural variants (SVs), repeat expansions, single-nucleotide variants (SNVs), and small insertions or deletions (Indels), with over a hundred genes and loci implicated in the pathogenesis of numerous neuromuscular disorders [8–10].

The heterogeneous genetic and epigenetic etiology of hypotonia-associated diseases, along with factors such as age of onset and neuroanatomic localization, contribute to a broad spectrum of phenotypes or clinical manifestations [11]. This complexity makes identifying the actual cause of hypotonia and/or muscle weakness quite challenging and significantly complicating the diagnostic journey and diminishing the likelihood of getting an accurate and early diagnosis and prognosis.

While whole-exome sequencing (WES) and short-read whole-genome sequencing (SR-WGS) have significantly advanced the diagnosis of rare genetic diseases, these approaches still encounter notable challenges in capturing critical genetic aberrations such as complex SVs, repeat expansions, and epigenetic modifications, which are critical diagnostic determinants for different types of hypotonia-associated diseases [12]. Consequently, current diagnostic workflows often involve sequential testing paradigms, which include methylation-specific multiplex ligation-dependent probe amplification (MS-MLPA) and chromosomal microarray analysis (CMA) for imprinting disorders [3], as well as disease-specific targeted assays such as droplet digital PCR (ddPCR) for SMA, triplet repeat-primed PCR (TP-PCR) for DM, and methylation-specific triplet-repeat PCR (TR-PCR) for FXS [13–16].

Third generation long-read sequencing (LRS) technologies offer a potential solution. By generating reads spanning from 1 kb to over 2 Mb, LRS enables the accurate detection of complex SVs and repeat expansions while simultaneously profiling CpG methylation status within a single assay [17, 18]. However, the clinical utility and cost-effectiveness of a first-tier LRS approach remain unproven, particularly in a pediatric cohort with hypotonia and muscle weakness, where these variants are a common cause of disease.

To address this gap, we established a unified, comprehensive diagnostic approach for patients exhibiting unexplained hypotonia or muscular weakness using LRS technology. We first characterize the current standard-of-care diagnostic approach and its associated limitations in a cohort of hypotonic patients. We then develop and optimize a long-read whole-genome sequencing (LR-WGS) protocol, paired with a comprehensive bioinformatics analysis pipeline targeting hypotonia-related loci, to simultaneously detect genomic variants and epigenetic alterations as a single-step diagnostic tool using DNA samples from patients representing 6 different hypotonia-associated diseases. Finally, we assess the clinical

utility and potential testing and healthcare cost savings of our approach by sequencing undiagnosed patients manifesting unexplained hypotonia.

Methods

Study cohort

The retrospective cohort analysis consisted of 227 patients presenting with hypotonia and/or muscle weakness as their primary clinical symptom, along with various additional clinical manifestations. These patients were admitted to Al Jalila Children's Specialty Hospital (AJCH), Dubai, UAE. This analysis aimed to characterize diagnostic yield and time-to-diagnosis, detailing the complex, time-consuming sequential tests which patients experience during their diagnostic journey. A total of 15 patients with a confirmed diagnosis of FXS ($n=4$), MD ($n=2$), PWS/AS ($n=2$), SMA ($n=4$), or DMD ($n=3$) were selected as the positive reference group for the optimization and validation of the LR-WGS with targeted (in silico) analysis. The clinical utility of this approach was evaluated in 14 patients with unexplained hypotonia and negative WES results (Fig. 1). All patients or their guardians consented to clinical genetic testing. This study was reviewed and approved by the Dubai Scientific Research Ethics Committee, Dubai Health Authority (approvals no. DSREC-SR-05/2024_03 and DSREC-08/2024_09).

DNA isolation

Genomic DNA (gDNA) from patient whole blood samples was extracted using the Qiagen DSP DNA kit and the QIAsymphony automated nucleic acid extraction system (Qiagen, Germany). DNA quality and purity were assessed using a NanoDrop One Microvolume UV–Vis Spectrophotometer and Invitrogen Qubit dsDNA broad-range quantification assay kit (Thermo Fisher Scientific, USA).

Clinical genomic workup

Clinical genomic testing was performed in the 227 retrospective patients and 15 positive reference group as previously described [19]. Clinical WES was performed using the Agilent Clinical Research Exome (CREv2) capture probes and the SureSelect^{XT} for library preparation (Agilent, USA), followed by (2 × 150 bp) sequencing to an average depth of 100 × on the NovaSeq6000 system (Illumina, USA). A custom bioinformatics pipeline was used for variant calling, annotation, filtration, and classification following the ACMG guidelines [20]. Chromosomal microarray was performed using the Affymetrix CytoScanHD system and the Chromosome Analysis Suite (ChAS) (Thermo Fisher Scientific, USA). Targeted genetic testing included droplet digital PCR for *SMN1* and *SMN2* copy number analysis (Bio-Rad, USA), triplet repeat (CGG) expansion analysis in the promoter region of the *FMR1* gene using the FragileX AmplideX® PCR kit (Asuragen, USA), and capillary electrophoresis (Thermo Fisher Scientific, USA), and methylation-specific multiplex ligation-dependent probe amplification (MS-MLPA) for PWS/AS (MRC-Holland, The Netherlands).

Library construction and long-read sequencing (LRS)

Sequencing libraries were constructed from 1.5 to 2 µg of high-molecular-weight genomic DNA, which was sheared to a target size of 8–12 kbp. Libraries were prepared using the Oxford Nanopore Ligation Sequencing Kit V14 (SQK-LSK114) for human samples, following the manufacturer's protocol, including DNA repair, end-prep, and adapter ligation steps. Each library was sequenced on a PromethION R10.4.1 flow cell using a PromethION 48 instrument, targeting ~ 30 × genome-wide coverage. Sequencing runs were conducted over 72 h, with a flow cell wash and library reload performed at the 24-h mark. Basecalling was performed in real-time using MinKNOW software (v24.06.14). Comprehensive technical details, including centrifugation parameters and catalog numbers, are provided in the Additional file 1.

Basecalling and primary long-read data analysis

Basecalling and simultaneous 5mC/5hmC detection were performed using Guppy (v.6.1.5). Low-quality reads (Q score < 9) were filtered to ensure call accuracy. All passing FASTQ files were aligned to the human reference genome (GRCh38) using minimap2 (v.2.28). The primary analysis was carried out using an Epi2Me workflow wf-human-variation (v.2.6.0) [21]. Small variants, including single-nucleotide variants (SNVs) and indels, were called using clair3 (v.1.0.4). Structural variants (SVs) were identified using Sniffles (v.2_2.0.7) [22] and CuteSV (v.2.1.1) [23]. Short tandem repeats (STRs) were genotyped using Straglr (v.1.4.5). Copy number variants (CNVs) were called with QDNASeq (v.1.34.0), and methylation was called using modkit. Additional details are provided in the Additional file 1.

Filtering and prioritization of structural and copy number variants (SVs and CNVs)

A stepwise filtering approach was applied to downstream analysis to identify putative pathogenic SVs and CNVs in our cohort. Initially, the analysis commenced with the identification of high-quality variants that met defined quality-control parameters (see Additional file 1 for details). SVs and CNVs that passed these thresholds were annotated using RefSeq gene annotations from the GRCh38.p14 reference (GCF_000001405.40), which

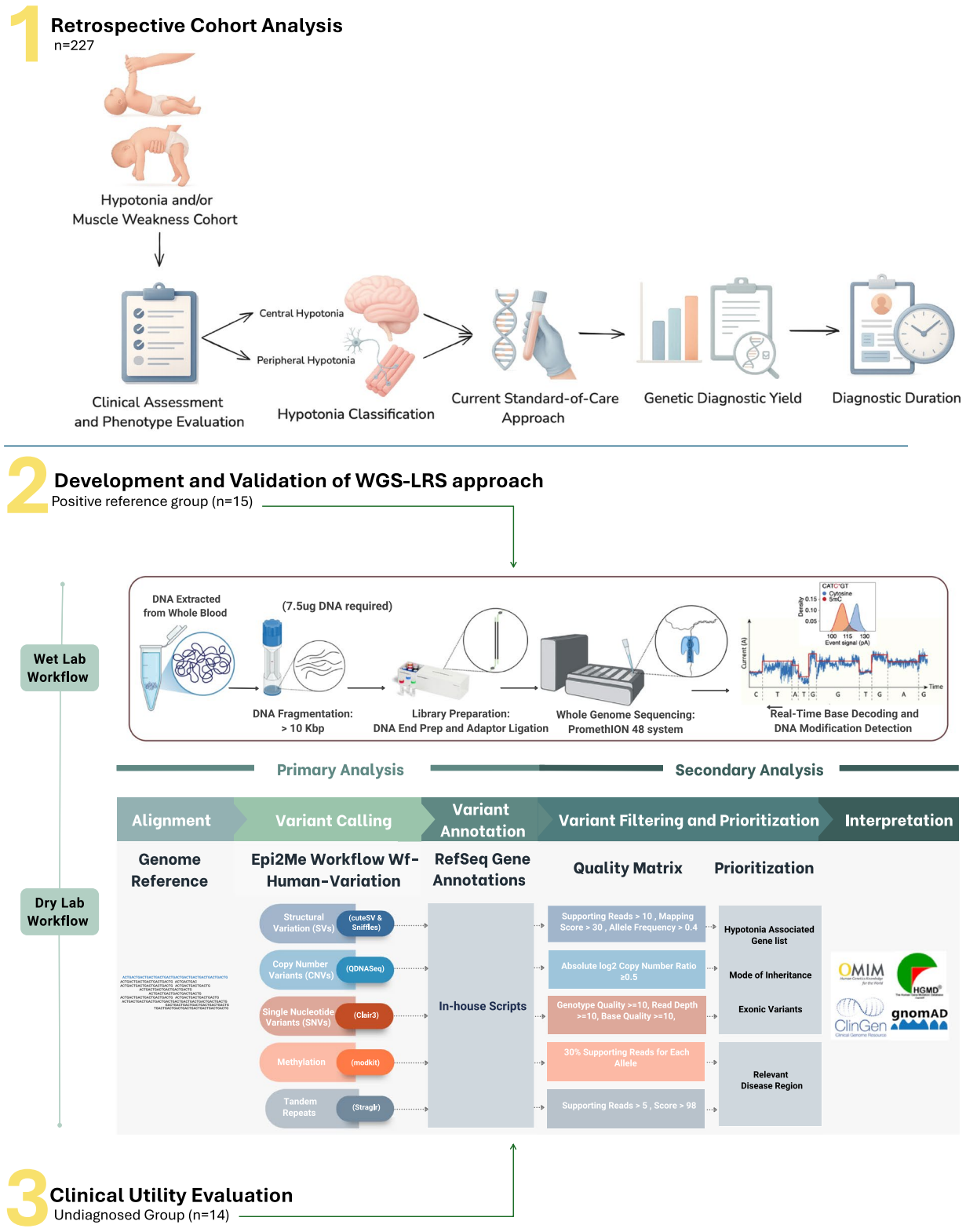

Fig. 1 Overview of the study design and workflow. The study consisted of three main steps: (1) retrospective cohort analysis ($n = 227$), including clinical evaluation, hypotonia classification, standard-of-care genetic testing, diagnostic yield, and time-to-diagnosis; (2) development and validation of the LR-WGS workflow ($n = 15$), covering both wet lab procedures and dry lab analysis with the tools used; and (3) Evaluation of clinical utility ($n = 14$) using the optimized workflow

includes exon and intron information for protein-coding genes. To facilitate variant interpretation and prioritization, gene-specific inheritance data were incorporated from the Human Gene Mutation Database (HGMD), Online Mendelian Inheritance in Man (OMIM) [24], and the Gene Curation Coalition (GeneCC) [25].

We then focused on genes with known associations to hypotonia-related disorders, using a curated list of 165 genes (Additional file 1). This list comprised 122 genes routinely analyzed in the clinical diagnostics workflow at Al Jalila Children's Hospital and 43 additional genes sourced from the published literature on muscular dystrophies [26]. Within these genes, the analysis prioritized exonic variants due to their greater potential to disrupt protein structure or function and thus confer pathogenicity. Subsequently, we filtered variants based on zygosity to match the known inheritance pattern of each gene, excluding, for instance, heterozygous variants in autosomal recessive genes unless a second pathogenic allele was detected.

All candidate SVs and CNVs were visually validated using the Integrated Genomics Viewer (IGV). The final interpretation of candidate variants considered their protein effects, disease mechanisms, inheritance modes, and supporting evidence from established variant databases, including ClinVar [27], ClinGen [28], OMIM [24], and HGMD.

Small nucleotide variants (SNVs and indels)

To identify pathogenic SNVs and indels, variant analysis was limited to a curated panel of genes associated with hypotonia, restricted to coding regions and canonical splice sites, and annotated for functional consequences. All candidate variants were functionally annotated using the RefSeq database to classify their molecular consequence (e.g., nonsense, frameshift, missense, or splicing variants). Variants were then prioritized based on zygosity and mode of inheritance consistent with the implicated gene, using information from the HGMD, OMIM, and GeneCC. Finally, variants classified as pathogenic or likely pathogenic were retained for phenotype–genotype correlation analysis (Additional file 1).

Short tandem repeat (STR) expansions

To identify pathogenic STR expansions in coding or non-coding regions, we focused on pathogenic STR loci associated with hypotonia and/or muscle weakness, such as FXS, myotonic dystrophy 1 (DM1), and myotonic dystrophy 2 (DM2). STRs were classified as "Normal", "Full-Mutation" which represents the pathogenic expansion, or "Pre-mutation," which contains repeat counts ranging between the upper limit of the normal range and the lower limit of the pathogenic range. To ensure analytical reliability, we restricted our interpretation to high-confidence STR calls by selecting alleles that are supported by at least 30% of the sequencing reads. This threshold was applied to minimize false positives and ensure accurate repeat sizing.

Methylation analysis

To investigate DNA methylation patterns associated with hypotonia and/or muscular weakness, we focused on specific genomic regions implicated in known imprinting and methylation-sensitive disorders. These included loci associated with PWS/AS at 15q11.2, specifically the CpG77 region (chr15:24,954,888–24,955,907) [29]. We also examined methylation signatures relevant to SMA, targeting the *SMN1* (chr5:70,944,127–70953338) and *SMN2* (chr5:70,074,524–70077354) regions, as recently described by Sinha et al. [30] [30]. For FXS, methylation levels were assessed at the *FMR1* promoter region (chrX:147,911,892–147,912,180), providing an epigenetic biomarker for FXS diagnosis [31]. Only methylation calls supported by a minimum of five reads and a quality score exceeding 98 were retained for downstream analysis to ensure high-confidence results.

Orthogonal validation

The heterozygous *COL6A3* deletion was confirmed experimentally using PCR with primers designed to target the genomic regions upstream and downstream of the deletion (COL6A3-del-Fwd: 5′-AAGCCAGGAAAC CCTCACAA-3′; COL6A3-del-Rev: 5′-TTAAAGGTC ACCTGCTGC-3′). PCR was performed using genomic DNA from the proband, both parents, and an unaffected patient (control). Reactions were analyzed by gel electrophoresis and visualized (Additional file 1).

Test cost analysis and economic utility

The cost of the current standard-of-care testing, which includes both multi-test and single-test diagnostic pathways, for our cohort ($n=227$) was compared to that of a single-tier LR-WGS-based approach with targeted (in silico) analysis. Institutional costs for each test were as follows: CMA: $1014; Single WES: $1972; Trio WES: $3199; Targeted NGS panel: $1299; DMD: $849; Fragile X TR-PCR: $199; SMA copy number analysis: $583; and PWS/AS methylation and deletion and duplication analysis: $800. These costs include laboratory markup, computational analysis, clinical interpretation and reporting, and institutional overhead. Costs were initially obtained in local currency and converted to U.S. dollars (USD) using the average 2025 exchange rate. Costs were assigned to each patient according to the tests they received and summed across all patients to obtain the total standard-of-care cost. Cost data were analyzed using descriptive statistics,

including mean, range, and total costs per patient and per diagnostic strategy.

For the LR-WGS based pathway, a fixed cost of $1500 per patient was calculated, including marked-up sequencing reagents and consumables ($800), technician hands-on labor ($100), targeted bioinformatics analysis and clinical reporting ($400), and institutional overhead ($200). It is important to note that, although LRS involves WGS, analysis is only targeted to hypotonia loci (similar to targeted NGS panels), thus significantly reducing analysis and reporting time, which generally incur high costs for comprehensive genome-wide analysis (e.g., CMA and WES) where bioinformatics analysis and clinical interpretation contribute meaningfully to the observed cost difference. Two test cost comparisons were performed: (i) the observed cost of the multi-test approach for patients diagnosed through multiple assays versus the projected cost if the LR-WGS based approach had been implemented as the first-tier test, and (ii) the total cost of standard-of-care testing for the entire cohort versus the projected total cost if the LR-WGS based approach had been applied to all patients.

To estimate the economic utility of the anticipated shortened time-to-diagnosis by LR-WGS, the cost of delayed diagnosis was first estimated using published data for eight rare diseases reported by the EveryLife Foundation for Rare Diseases [32] [32], including adrenoleukodystrophy (ALD), infantile-onset and late-onset Pompe disease, Severe Combined Immunodeficiency (SCID), FXS, DMD, Wilson Disease, generalized Myasthenia Gravis female (gMG-F), and generalized Myasthenia Gravis male (gMG-M). Using these data, the average annual cost per disease was calculated. This was subsequently used to estimate the average delayed diagnostic cost per year across the eight diseases, which was then applied to the 29 patients in our study who eventually received a diagnosis under the multi-test approach to estimate the cost of delayed diagnosis due to the standard-of-care sequential testing.

Results

The diagnostic journey of patients with hypotonia and/or muscle weakness

Of the 227 patients, 120 (53%) were females, and the majority (220/227 or 97%) were pediatric patients, with a median age at first clinical presentation of 1 year (range: newborn to 48 years). Clinical evaluations revealed that approximately 67% of patients ($n=152$) were suspected to have peripheral hypotonia, while 16.3% ($n=37$) were suspected to have central hypotonia. The remaining cases were classified as having mixed features or non-specific/generalized hypotonia, accounting for 3.5% ($n=8$) and 13.2% ($n=30$), respectively (Fig. 2a, Additional file 2: Table S1–S2). This classification shows considerable clinical variability among patients exhibiting a wide range of neurological and neuromuscular manifestations associated with hypotonia, reflecting the complexity of this phenotype.

Genetic testing in this cohort yielded a molecular diagnosis in 95 patients (42% overall diagnostic yield), while more than half of the patients ($n=132$ [58%]) remained without a definitive diagnosis (Fig. 2b, Additional file 2: Table S1–S2). In-depth analysis revealed marked heterogeneity in diagnostic pathways among these patients, reflecting notable variability in the types and numbers of genetic tests administered to each patient (Fig. 2c, Additional file 2: Table S1–S3). Genetic testing modalities used in this cohort included CMA, WES, NGS gene panels (for myopathies or MDs), and targeted testing for SMA (by ddPCR), fragile X (TR-PCR), and methylation analysis (MS-MLPA) for PWS/AS (Fig. 2c).

The diagnostic yield varied among patients who received single versus multiple tests (Fig. 2b). Among patients who received single tests ($n=166$), 66 (39.8%) had a definitive diagnosis, accounting for 29.1% of total diagnostic outcomes. Of the single tests, targeted SMA testing was the most frequently utilized ($n=102$), achieving a diagnostic yield of 44% (45/102) in this group, followed by other tests, such as WES (5/21; 24% yield), multi-gene panels (12/20; 60% yield), CMA (3/19; 16% yield), and MLPA (1/4; 25%) (Fig. 2c, Additional file 2: Table S3).

Of all patients in this cohort, 61 underwent multiple sequential investigations that reached up to four different tests. The multi-test approach achieved 29 diagnoses (47.5%) and contributed ~ 12.8% of the total diagnostic yield (Fig. 2b, Additional file 2: Table S3). Interestingly, 19 unique test combinations were documented in this subset. The most frequently employed combination of tests, CMA and WES ($n=14$), alongside SMA and targeted gene panel combinations ($n=13$), showed varied diagnostic yields (Fig. 2c).

LR-WGS for comprehensive genomic and epigenomic profiling of hypotonia patients

Utilizing LR-WGS, we developed a diagnostic approach for simultaneous examination of a broad spectrum of genomic variants and epigenetic alterations, including SVs, CNVs, STRs, SNVs, Indels, and DNA methylation changes within hypotonia-associated genes. The validation of this approach was conducted on a positive reference group consisting of patient samples ($N=15$) with previously confirmed genetic diagnoses linked to hypotonia. These diagnoses were established through traditional methods, including MLPA, PCR, methylation analysis, CMA, WES, and targeted NGS panels (Fig. 3a, Additional file 2: Table S4).

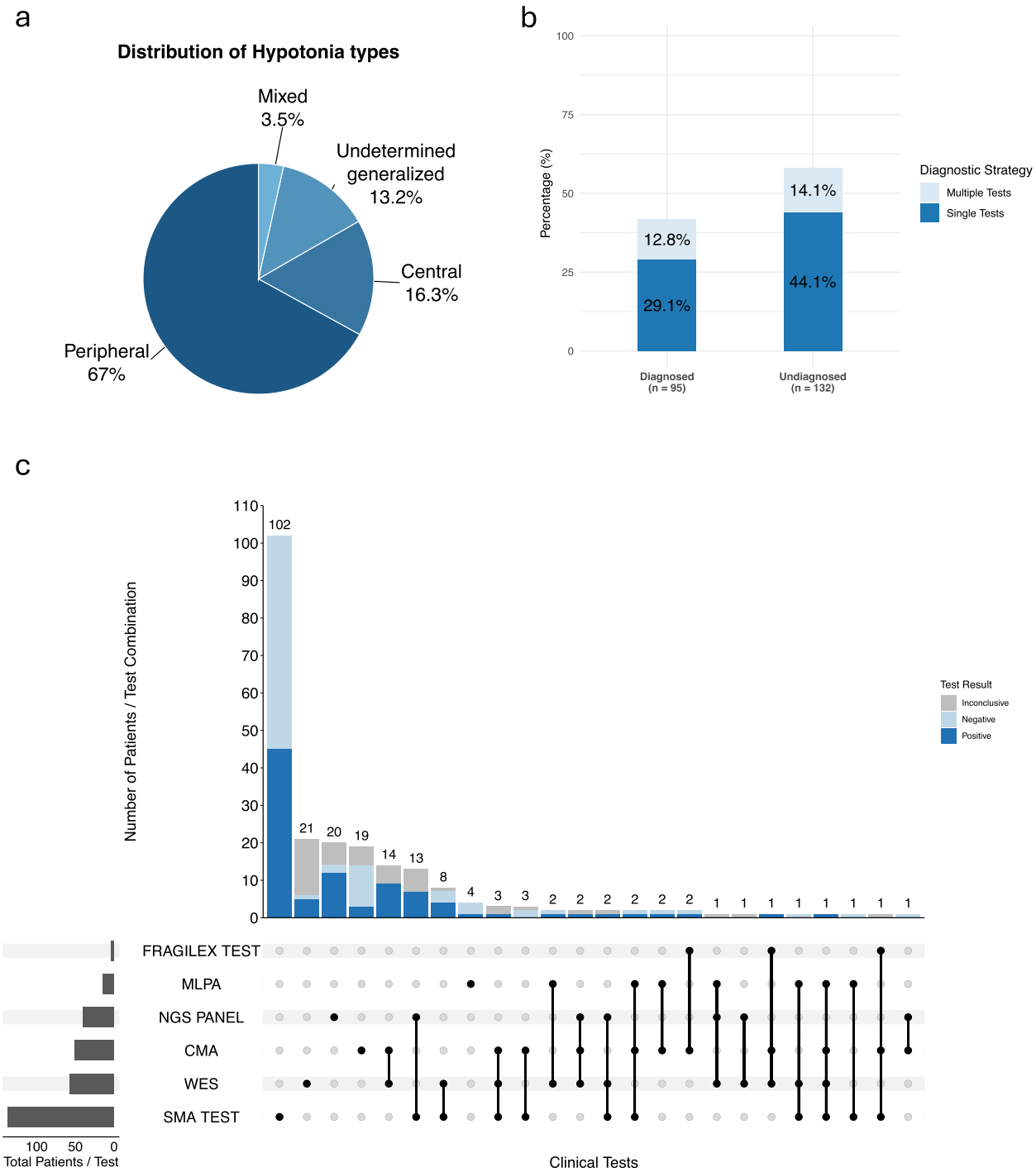

Fig. 2 Overview of the hypotonia cohort analysis. **a** Clinical classification of hypotonic patients based on associated symptoms. **b** Diagnostic yield of single-test vs. multi-test approach, with diagnostic and undiagnostic percentages shown relative to the total cohort. **c** UpSet plot illustrating combinations of traditional diagnostic tests performed and their frequency among the hypotonia cohort. Each vertical bar represents a unique test combination; filled dots indicate which tests were included. Bar height reflects the number of patients who underwent that combination, with the number of patients annotated above each bar. Horizontal bars (left) represent counts of each test used solo or in combination with other tests

a

Sample	Diagnosis	Genetic Mechanism	Clinical Test Performed
FFX-01	Fragile X Syndrome	Full mutation (>200 repeats)	The CGG triplet PCR
FFX-02	Fragile X Syndrome	Full mutation (>200 repeats)	The CGG triplet PCR
PFX-01	Fragile X Syndrome carrier	Premutation (96,30)	The CGG triplet PCR
PFX-02	Fragile X Syndrome carrier	Premutation (98,30)	The CGG triplet PCR
DMD-01	Duchenne Muscular Dystrophy	Deletion in exon 8 and 9 (*DMD* gene)	WES
DMD-02	Duchenne Muscular Dystrophy	Deletion in exon 44 (*DMD* gene)	MLPA
DMD-03	Duchenne Muscular Dystrophy	Deletion in exon51-55 (*DMD* gene)	MLPA
DM-01	Muscular Dystrophy	One heterozygous pathogenic variant (Gln656*) in *DMD* two heterozygous VUSs in *CLCN1* and *MYH2*	Targeted NGS panel
DM-02	Muscular Dystrophy	Homozygous pathogenic variant (Leu307fs) in *SGCA*	Targeted NGS panel
PWS-01	Prader Willi Syndrome	Deletion in PWS imprinting center region (ICR) and epimutation in the parental chromosome	MS-MLPA
AS-01	Angelman Syndrome	15q LOH and UPD	MS-MLPA
SMA-01	Spinal Muscle Atrophy	Homozygous deletion of exon7 in *SMN1* gene	Digital Droplet PCR
SMA-02	Spinal Muscle Atrophy	Homozygous deletion of exon7 in *SMN1* gene	Digital Droplet PCR
SMA-Carrier-01	Spinal Muscle Atrophy carrier	Heterozygous deletion of exon7 in *SMN1* gene	Digital Droplet PCR
SMA-Carrier-02	Spinal Muscle Atrophy carrier	Heterozygous deletion of exon7 in *SMN1* gene	Digital Droplet PCR

b

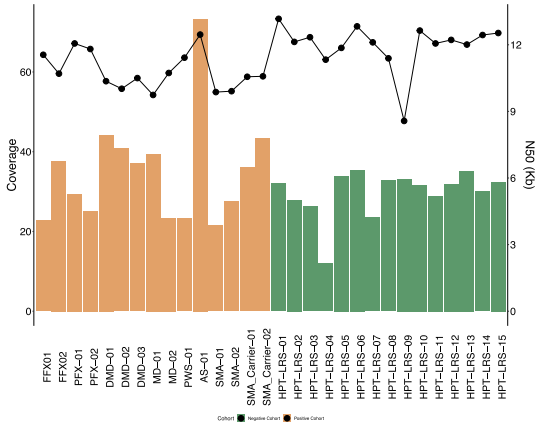

Fig. 3 Characterization of the positive cohort and nanopore sequencing quality. **a** Table summarizing the clinical diagnoses of individual samples in the positive cohort, along with the clinical assays used to confirm each diagnosis. **b** Quality metrics from Nanopore WGS, with N50 read length represented by lines and genome coverage by bars

The LR-WGS protocol applied to this cohort generated approximately 73 Gb to 142 Gb of data per sample with high-quality reads, featuring a median N50 read length of approximately 10.81 kb (range: 9.74 kb to 12.46 kb), and resulting in a median genome-wide coverage of around 34.9× (range: 21.50× to 73.33×) (Fig. 3b, Additional file 2: Table S4). This level of coverage was required to enable effective variant calling across various regions using a bioinformatics workflow with in-depth analysis of both genetic and epigenetic alterations.

An optimized stepwise filtering pipeline was developed to prioritize clinically relevant SVs and CNVs associated with a curated list of hypotonia-related genes (Additional file 2: Table S5), while adhering to established quality metrics (Fig. 1 and " Methods"). This approach facilitated the selection of high-confidence exonic variants and resulted in a significant reduction of identified raw variants by 97.9% for CNVs and 99.9% for SVs, yielding an average of 1 to 6 high-confidence SVs/CNVs per sample (Fig. 4a, Additional file 2: Table S6). Among this collection of confidently identified SVs and CNVs, all known pathogenic multi-exon deletions in the *DMD* gene, previously identified in DMD patients, were retained. Moreover, we detected a heterozygous deletion within the PWS imprinting control region (ICR) in a positive sample diagnosed with PWS (PWS-01) through CNV analysis (Fig. 4b). On the other hand, DNA methylation pattern analysis of the 15q11.2–q13 PWS/AS imprinted locus revealed the expected aberrant hypermethylation patterns in the same patient, which aligned with the molecular diagnosis results obtained from MS-MLPA (Fig. 4c). Furthermore, methylation profiling of this region in the patient diagnosed with AS (AS-01) revealed copy number-neutral hypomethylation, consistent with the absence of the maternal allele (Fig. 4c) due to paternal uniparental disomy (pUPD) or an imprinting defect.

The DNA methylation analysis in this assay included an investigation of the SMA-specific methylation tag at the *SMN1/SMN2* locus, as recently characterized by our group [30]. This analysis aligns with the expected methylation profile across the cohort (Fig. 4d). In patients with SMA, we observed a complete loss of methylation downstream of exon 6, consistent with a homozygous deletion of exon 7 in the *SMN1* gene. In SMA carriers with one functional *SMN1* copy, partial methylation was detected, with approximately 50–70% of bases methylated. In contrast, all unaffected individuals exhibited complete methylation (100%) at this locus, confirming their unaffected status.

We subsequently assessed the capability of our pipeline to detect known pathogenic repeat expansions. We genotyped STRs from the LR-WGS data across a variety of clinically significant STR-associated genes. This approach facilitated a thorough evaluation of 33 disease-associated loci, including the primary targets relevant to this study: *FMR1* (associated with Fragile X syndrome), *DMPK*, and *CNBP* (linked to myotonic dystrophy types 1 and 2). The expanded alleles were accurately categorized into full mutation and premutation ranges based on the estimated repeat counts.

The pathogenic CGG trinucleotide expansions located in the 5′ UTR of *FMR1* were identified in two clinically diagnosed Fragile X patients (FFX-01 and FFX-02), while premutation alleles were detected in two carriers (PFX-01 and PFX-02) within the positive reference group (Fig. 4e). Normal allele ranges in *FMR1* and

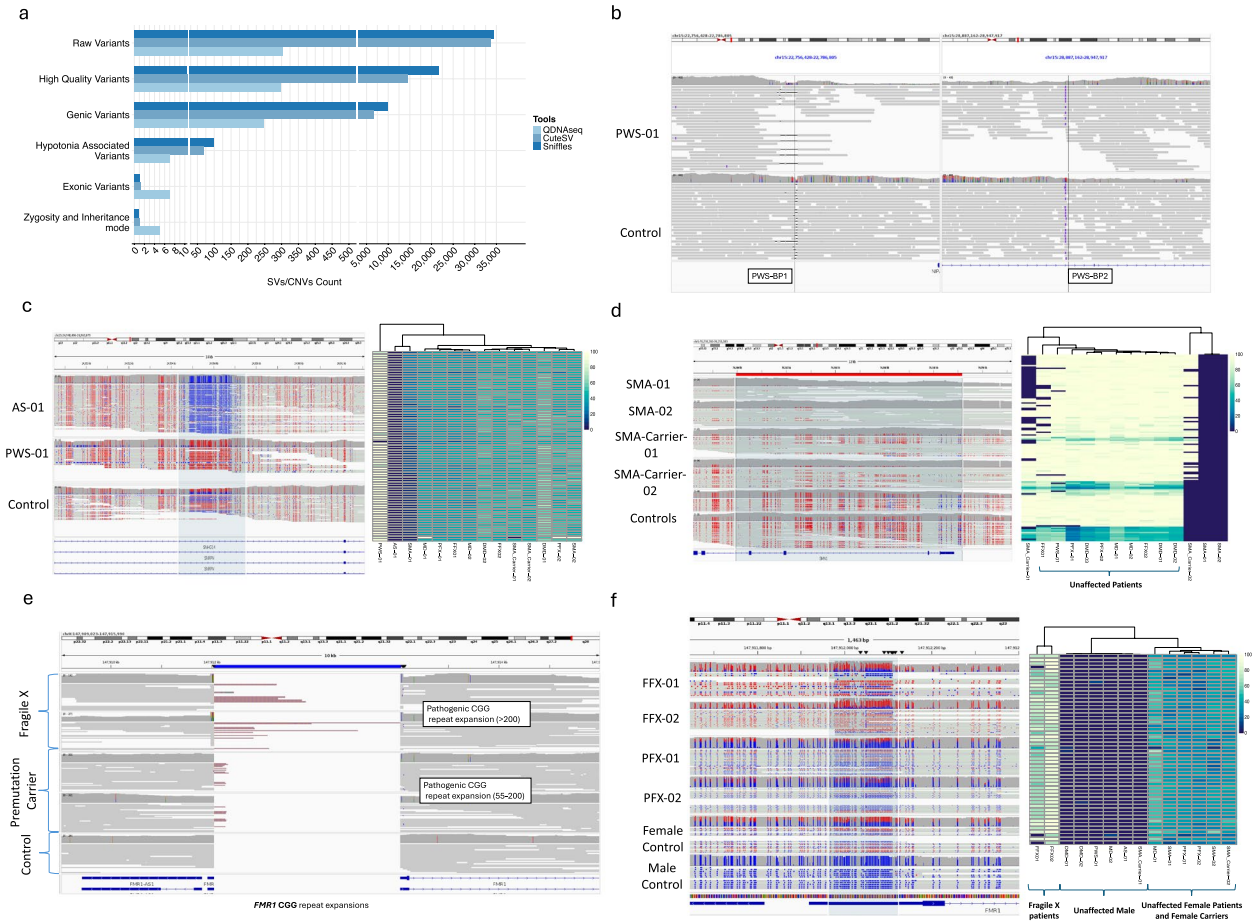

Fig. 4 Comprehensive genomic and epigenomic variant profiling in the positive cohort using long-read sequencing. **a** Variant filtering summary: Bar plot showing average variant counts at each filtering step among the positive cohort using three structural variant callers: cuteSV, Sniffles, and QDNAseq. **b** PWS deletion breakpoint visualization: IGV screenshots showing two breakpoints flanking a large microdeletion within the PWS imprinting control region (ICR) in a PWS patient. Compared to the control, the PWS sample exhibits reduced coverage and loss of heterozygosity between the two breakpoints (BP1 and BP2), supporting a heterozygous deletion. **c** Methylation profile of the PWS/AS imprinting region: Right, heatmap showing base-level methylation (%) across the 15q11.2–q13 region. Each column represents an individual sample, color intensity reflects the methylation percentage at each CpG site (0% = hypomethylation, 100% = hypermethylation). Left, IGV methylation tracks from a PWS patient (PWS-01), AS patient (AS-01), and a control, with methylated bases in red and unmethylated bases in blue. **d** SMA methylation tagging: Right, heatmap showing base-level methylation (%) across the *SMN1* region (chr5:70,239,954–70249165). Left, IGV methylation profiles for SMA patients (SMA-01, SMA-02), carriers, and controls. **e** CGG repeat expansion in *FMR1*: IGV screenshots showing long-read alignments at the *FMR1* promoter, highlighting CGG repeat expansions in Fragile X patients (FFX-01, FFX-02), carriers (PFX-01, PFX-02), and a control. Repeat lengths vary by clinical status, with full mutations showing > 200 expansion and intermediate mutation showing 55 to 200 expansion. **f** *FMR1* promoter methylation: right, heatmap of methylation (%) at the *FMR1* promoter (chrX:147,911,892–147,912,180). Left, IGV views of methylation patterns in Fragile X patients, carriers, and male/female controls

STR-associated loci were also accurately identified, providing comprehensive repeat profiling. LR-WGS also detected the methylation status at the *FMR1* promoter region (Fig. 4f), revealing hypermethylation in patients with a full CGG expansion (FFX-01 and FFX-02). This finding is consistent with the expected epigenetic silencing of the gene and the presence of severe clinical phenotypes. Conversely, carriers of premutation alleles (PFX-01 and PFX-02) exhibited partially methylated profiles, indicating a lack of transcriptional silencing (Fig. 4f). As anticipated, male controls displayed a fully unmethylated *FMR1* promoter profile, while female controls showed both methylated and unmethylated reads at the *FMR1* promoter region (Fig. 4f), which aligns with the dynamics of X-chromosome inactivation. Additionally, among all unaffected individuals in the reference cohort, the methylation profiles remained within normal ranges.

A stepwise filtering process focusing on stringent quality control metrics and selection of annotated exonic and intronic SNVs/indels with significant predicted functional

impact within genes associated with hypotonia (Fig. 1 and " Methods") successfully identified previously reported heterozygous and homozygous SNVs/indels in the *DMD*, *CLCN1*, *MYH2,* and *SGCA* genes in patients MD-01 and MD-02 (Fig. 3a). The concordance of SNV and indel calls generated by LRD was assessed by comparing all these calls, regardless of pathogenicity, with SRS within hypotonia-associated genes across eight samples that had previously undergone WES. Prior to quality control filtering, an average concordance rate of approximately 90% was observed across the eight samples (Additional file 3: Fig. S1, Additional file 2: Table S6). Following the application of stringent quality control filters, the concordance rate between the two technologies was, on average, 95% while the proportion of discrepant calls decreased to an average of 2% (Additional file 3: Fig. S1).

Clinical utility of the LR-WGS based approach in Undiagnosed Patients

Diagnostic increment

To evaluate the diagnostic potential of the LR-WGS based approach, we applied this comprehensive method to a cohort of 14 patients who had previously undergone standard-of-care WES but had not achieved a definitive molecular diagnosis. LR-WGS protocol applied to this cohort generated approximately 75 Gb to 113 Gb of data per sample, with a median N50 read length of 12.02 kb (range: 8.57–13.17 kb) and an average coverage depth of 31×(range: 23.49×to 35.36×), demonstrating sufficient sequencing quality across all samples (Fig. 3b). Filtering high-confidence SVs and CNVs yielded a total of approximately 29 high-confidence SVs and 42 CNVs across all samples and reduced the number of raw variant calls by 99.9% for SVs and 98.9% for CNVs, respectively (Additional file 2: Table S6).

Among the final prioritized and filtered structural variants, a heterozygous 325 bp deletion in the *COL6A3* gene (GRCh38: g.237359304_237359629del; NM_004369.4(*COL6A3*):c.6283-241_6310-54del;P.?) was identified in a previously undiagnosed patient, HPT-05 (Fig. 5a). This deletion is expected to result in an in-frame deletion of exon 18, encoding 9 amino acids within the triple-helical (TH) domain of the α3(VI) collagen chain. The TH domain is a critical structural component of collagen VI, characterized by a repeating Gly-X–Y amino acid motif that is essential for the assembly of α1(VI), α2(VI), and α3(VI) chains into monomers and subsequently collagen VI tetramers prior to secretion into the extracellular matrix. Disruption of this domain is expected to allow the mutated chain to be integrated into the collagen VI tetramer, thereby exerting a dominant-negative effect on the collagen VI microfibril assembly and function [33]. *COL6A3* is associated with the autosomal dominant form of VI collagenopathy, including Bethlem Myopathy (BM, MIM# 158,810), which manifests as hypotonia, muscle weakness, and muscle atrophy, symptoms consistent with our patient's clinical presentation [34, 35]. Based on this finding, we manually analyzed the clinical WES data, which revealed a breakpoint and a reduction in coverage over exon 18 in the patient but not in either parent (Fig. 5b), confirming the de novo status of this deletion, a finding which was further validated by PCR and gel electrophoresis (Fig. 5c, Additional file 2: Table S7, Additional file 4). According to the ClinVar database, splicing variants that cause skipping of *COL6A3* exon 18 have been reported in patients with dominantly inherited disease, likely as a result of disruption of the triple-helical domain of collagen VI [33, 36, 37]. Taken together, the de novo deletion of exon 18 was classified as pathogenic and considered the cause of disease in patient HPT-05.

In patient HPT-12, a heterozygous duplication spanning approximately 835 kb (*chr8:43,080,001–43,915,001*; *GRCh38*) was identified. The patient is an 8-month-old male who presented with severe hypotonia and generalized muscle weakness with no family history. This duplication encompasses the entire *POMK* gene (Fig. 5d–e). The *POMK* gene is associated with limb-girdle muscular dystrophy-dystroglycanopathy and Walker–Warburg syndrome, both of which are inherited in an autosomal recessive manner. Accordingly, the clinical significance of this duplication alone remains uncertain. However, methylation analysis of the *POMK* gene revealed an aberrant methylation signature at the promoter region, distinct from that observed in the remaining cohort ($n=13$) (Fig. 5e–f). Promoter hypermethylation is typically associated with transcriptional silencing. Nevertheless, more information is needed to determine the contribution of this genomic and epigenomic variation at the *POMK* locus in this patient. No other clinically relevant SNVs, SVs, CNVs, repeat expansions, or aberrant methylation patterns (Additional file 3: Fig. S2) were uncovered in other undiagnosed patients.

Shortened time-to-diagnosis

The diagnostic burden experienced by patient HPT-05, presented in infancy with a clinical picture of hypotonia, generalized muscle weakness, and severe proximal and distal muscle wasting, was considerable. The patient experienced a prolonged diagnostic journey involving two tests, WES and SMA copy number analysis, which ultimately ended without a defined diagnosis at the age of 3 years. However, upon undergoing LR-WGS, a precise diagnosis of *COL6A3*-related muscle

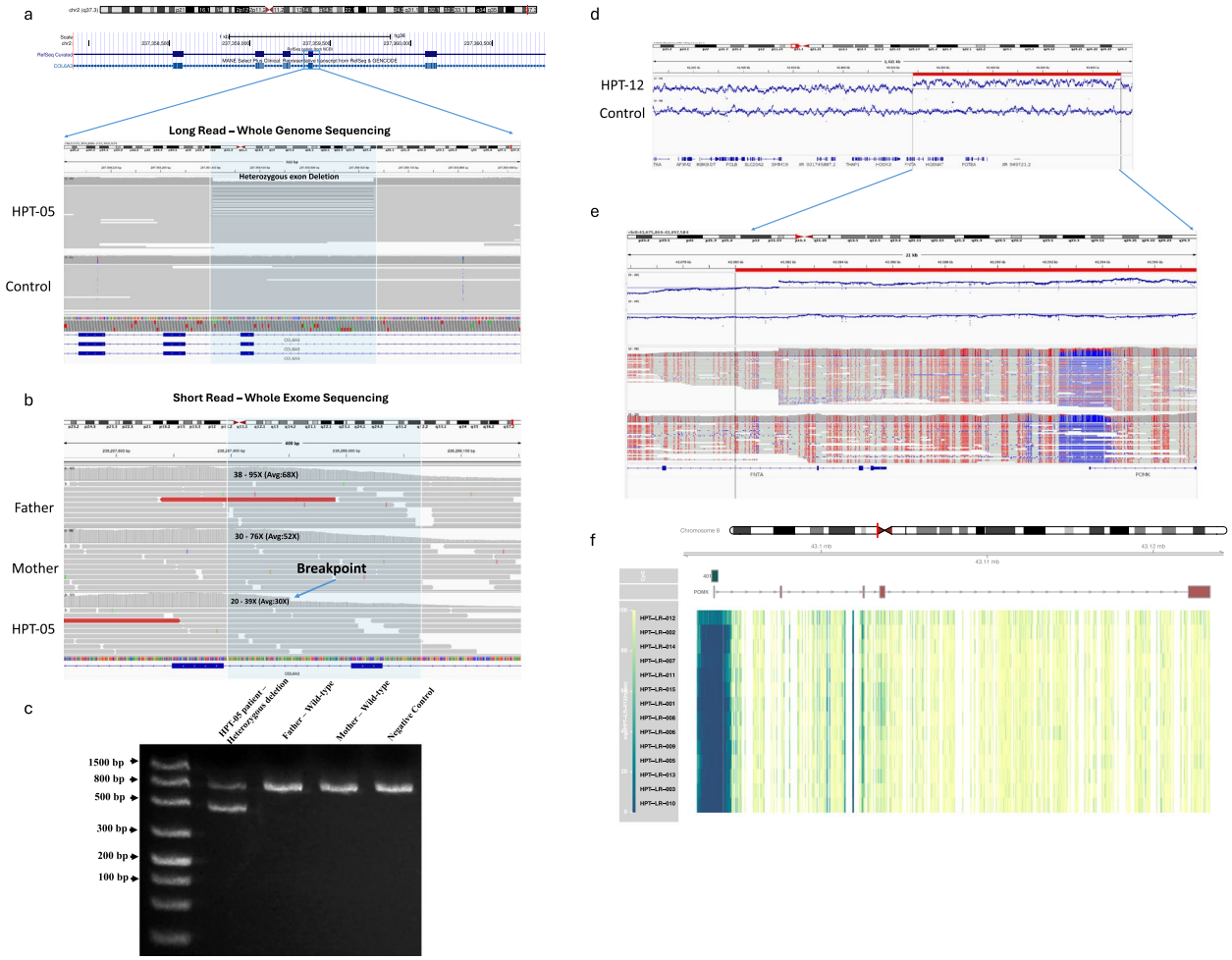

Fig. 5 Characterization and validation of genomic and epigenomic findings in undiagnosed patients. **a** IGV screenshots showing long-read alignments highlighting a heterozygous pathogenic deletion in patient HPT-05. **b** Coverage profiles from trio WES visualized in IGV, demonstrating a drop in read depth at the deletion breakpoint in the patient compared to both parents, consistent with a de novo event. **c** PCR gel electrophoresis of the *COL6A3* region in the proband (HPT-05), parents, and control. The lower molecular weight band in the proband corresponds to the deletion allele; the upper band indicates the wild-type allele, consistent with a heterozygous deletion. **d** IGV screenshots displaying long-read alignments in patient HPT-12. The red bar indicates the genomic region corresponding to the entire heterozygous duplication. Within this region, the increased read depth (blue alignments) in patient HPT-12 is evident compared to the reference sample, consistent with an additional copy (CN = 3). **e** IGV screenshots showing a detailed view of long-read alignments at the *POMK* promoter region, with methylated bases shown in red and unmethylated bases in blue. **f** Methylation profile of the *POMK* gene region: the heatmap showing base-level methylation (%) across the entire gene. Each row represents an individual sample, color intensity reflects the methylation percentage at each CpG site (0% = hypomethylation, 100% = hypermethylation)

disease was achieved within an estimated time of a few weeks.

The analysis of the diagnostic durations across the entire retrospective hypotonia cohort ($n = 227$, Fig. 6a) demonstrated a marked difference depending on the diagnostic strategy used: patients who received a diagnosis from the initial test ($n = 66$ or 70% of all diagnoses) had an average diagnostic duration of 24.8 days (range: 1 day to 3.42 months; note that this time increases significantly if we exclude SMA PCR testing which is relatively quick), whereas those who underwent a sequential testing approach ($n = 29$ or 30% of all diagnoses) had an average diagnostic time of 168.8 days (range: 14 days to 49.7 months), representing a statistically significant ($p < 0.001$, Mann–Whitney U test) delay in diagnosis (Fig. 6a, Additional file 2: Table S1). This indicates that the diagnostic approach has a substantial impact on time-to-diagnosis, with delays that may be avoidable through the use of a unified, comprehensive, LR-WGS based diagnostic workflow, which we estimate, based on the average

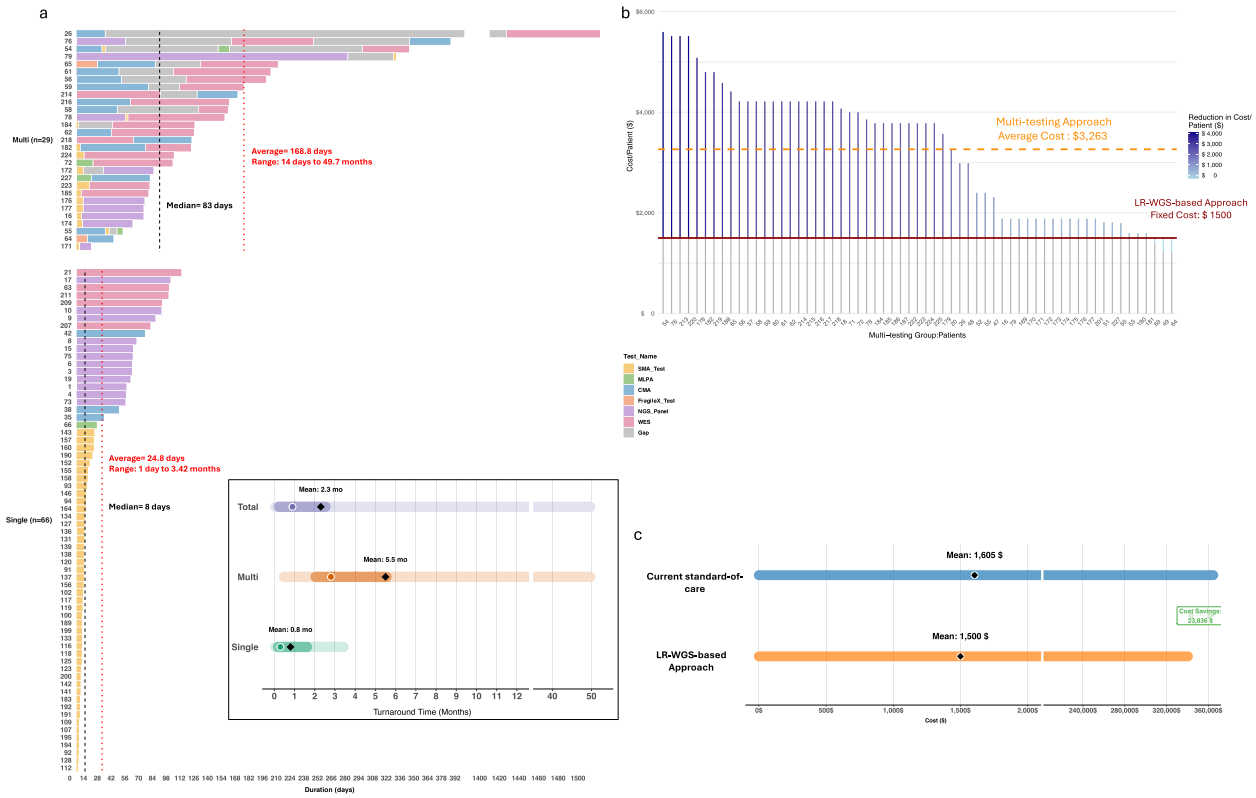

Fig. 6 Diagnostic time distribution and test cost impact. **(a)** Bar graph showing the diagnostic time distribution for patients with positive results, stratified by testing strategy. The *y*-axis represents the number of patients in single-test and multi-test groups. Colors indicate the diagnostic tests leading to the final diagnosis. The *x*-axis represents time to diagnosis in days. A black dashed line indicates the median time to diagnosis, and red dots represent the average time for each group. The lower graph represents average turnaround times for the diagnosed group ($n=95$) and those who received diagnostic single ($n=66$) or multi-testing ($n=29$). **b** Per-patient cost comparison between the current multi-testing and LR-WGS-based approaches. Vertical bars represent the total testing cost for each patient in the multi-testing group ($n=61$). The dashed orange line indicates the average cost of the current multi-testing approach ($3263), while the solid red line shows the fixed cost of the LR-WGS-based approach ($1500). The gradient coloring of the savings lines corresponds to the magnitude of cost reduction per patient. **c** Cohort-level cost comparison between the current standard-of-care and LR-WGS diagnostic approaches. Total cost of applying each diagnostic approach to the entire cohort ($n=227$). The length of the colored bar represents the total financial expenditure. The diamond markers represent the mean cost per patient for each strategy

turnaround time for a single test approach in our cohort, to be approximately 25 days, i.e., 85% reduction in time-to-diagnosis for patients who received multiple sequential testing. It is important to note that only 61 of the 161 patients with negative results after the first test (38%) underwent additional testing, implying that LR-WGS would have also benefited the remaining 100 patients (44% of the entire cohort) who could not undergo further testing for varied reasons.

Test cost and economic utility

The economic evaluation of the comprehensive LR-WGS-based diagnostic workflow demonstrated substantial advantages over the conventional multi-testing approach (Fig. 6b). Among patients who underwent multi-testing ($n=61$), testing costs exhibited considerable variability (range: $1213–$5596), with a mean cost of $3263 per patient and a total of $199,000. Based on the observed diagnostic yield of this pathway (47.5%), the corresponding cost-per-diagnosis was $6,864 (total cost divided by 29 diagnosed patients). In contrast, at a cost of $1500 per patient (Methods), the LR-WGS-based approach would lead to an average savings of $1763 per patient, corresponding to a 54% reduction in testing expenses in this group. The cost-per-diagnosis ($3155) would also be significantly lower, though it remains likely an overestimate, as it does not account for the potentially higher diagnostic yield associated with LRS.

When applied to the entire study cohort ($N=227$), where total genomic diagnostics cost was $364,336 (Methods), the LR-WGS based workflow was projected to reduce overall diagnostic costs by 6.5% ($23,836), yielding total savings of $105 per patient (Fig. 6c, Additional file 2: Table S8). Moreover, given the diagnostic

yield in the entire cohort (42%), the corresponding cost-per-diagnosis was $3835, while the cost-per-diagnosis for the LRS would be $3584. It is important to note that these direct cost comparisons do not take into consideration the (1) LRS enhanced diagnostic yield, which will further reduce the cost-per-diagnosis as well as the healthcare costs due to prolonged diagnostic odysseys (below), and [2] the reduced costs associated with operating a consolidated laboratory workflow using a single LRS platform compared to standard-of-care multi-test and multi-technology platforms requiring significantly higher capital investment, multiple quality management programs and a diverse pool of trained personnel.

In addition to test cost savings, we assessed the economic burden of prolonged diagnostic odysseys, which can be reduced by applying first-tier LRS diagnostic testing. For the 29 patients who underwent multi-testing, the total cumulative diagnostic duration was 13.4 years. Assuming a turnaround time of 25 to 42 days for LRS testing, consistent with that of standard targeted clinical panels, the total cumulative avoidable diagnostic delay in the multi-testing group would range from 10.37 to 11.50 years. Using the reported average annual healthcare cost of $38,223.49 attributable to diagnostic delays in individuals with rare diseases [32] (Methods), we estimate that the LR-WGS based approach may result in a reduction in economic burden of $396,208 to $439,527 due to avoidable diagnostic delays in those 29 patients.

Discussion

Here, we show that utilizing LR-WGS with targeted (in silico) analysis enables timely and comprehensive discovery of genomic and epigenomic variants in hypotonia and muscle weakness, improving diagnostic yield, shortening diagnostic timelines, and reducing costs compared with current standard-of-care testing.

LR-WGS demonstrated high sensitivity in detecting all previously known pathogenic variants, including SNVs, indels, CNVs, SVs, repeat expansions, and aberrant methylation profiles, while filtering out benign variants and artifacts, thereby alleviating the diagnostic burden and prioritizing clinically relevant variants associated with hypotonia. A significant advancement in this diagnostic approach is the simultaneous detection of genetic and epigenetic alterations, which adds substantial prognostic value and enables phenotype prediction and recurrence risk assessment in many cases. For example, not only can LR-WGS confirm a diagnosis in patients with Fragile X syndrome through the identification of fully expanded repeats in the promoter region of *FMR1*, but it can also determine the methylation status in this region, which is a critical factor to correlate with phenotype severity in patients with the disease [38]. Similarly, in addition to confirming a diagnosis of PWS/AS through the detection of abnormal methylation at 15q11.2, LR-WGS can pinpoint the exact cause of the disease and distinguish between a 15q11.2-q13 deletion, imprinting defect, and uniparental disomies (UPD), which have different implications for recurrence risk assessments and genetic counseling [39]. Such variation has generally been inaccessible to SRS and is typically detectable through specific targeted assays, which often lead to sequential testing approaches limited to a subset of patients and can be both costly and time-consuming.

The application of this approach to WES-negative hypotonia cases led to one definitive and one possible diagnosis in two out of 14 unresolved patients (14%). The de novo heterozygous deletion in the *COL6A3* gene, identified in patient HPT-05, confirms a molecular diagnosis of Bethlem myopathy (BM), which is a rare autosomal dominant disease on the milder end of the clinical spectrum of collagen VI–related myopathies characterized by a lack of distinct diagnostic features when compared to other muscular dystrophies or neuromuscular diseases [34, 40]. This makes early molecular confirmation especially difficult. This deletion was missed through the first-tier WES test, whereas sequential targeted testing strategies would likely have failed to detect the causal variant, as accurate identification would require direct copy number analysis of *COL6A3*, which is one of more than 40 genes implicated in muscular dystrophies presenting with overlapping phenotypes such as muscle weakness and hypotonia [41]. Therefore, this would ultimately have led to an extended diagnostic odyssey, increased costs, and, most likely, no definitive diagnosis. The use of a unified LRS approach enabled rapid, accurate variant detection, thereby avoiding these pitfalls. Importantly, a timely diagnosis in such cases is crucial for initiating targeted clinical interventions, including monitoring for progressive joint contractures and respiratory complications [42].

The importance of integrating genetic and epigenetic analyses within a unified diagnostic framework was further exemplified by the simultaneous identification of a heterozygous duplication of the *POMK* gene in patient HPT-12, along with an aberrant methylation signature at its promoter, a modification commonly associated with transcriptional silencing. Although the coexistence of increased copy number and promoter hypermethylation does not constitute a definitive molecular diagnosis, it raises the possibility of a complex regulatory mechanism whereby the additional genomic copy fails to increase gene expression due to epigenetic suppression. This observation may represent a previously underrecognized mechanism contributing to disease pathogenesis. Further investigations, including transcriptome profiling and

expression analyses, will be necessary to elucidate the functional consequences of this combined genetic and epigenetic alteration and to clarify its potential role in the proband's phenotype.

Our retrospective cohort analysis showed that many patients with hypotonia (58%) remained undiagnosed after standard-of-care testing, with limited access to further investigations, while those who underwent sequential testing typically faced an extended journey before achieving a definitive diagnosis. Interestingly, less than half of the undiagnosed patients (61/161 [38%]) were able to pursue additional testing, and of those, 29 (47.5%) eventually received a diagnosis. This suggests that additional testing could still have been useful for a large number of undiagnosed patients (>60%), though it was not pursued under current diagnostic paradigms, highlighting the significance of a unified, comprehensive diagnostic approach for hypotonia and muscle weakness. Delays in diagnosis for many of those patients impose high costs on healthcare systems, averaging $38,223 per year [32], underscoring that LR-WGS could yield far-reaching health economic benefits.

Furthermore, our analysis shows that the LR-WGS with targeted analysis represents a more cost-effective diagnostic strategy than current standard-of-care paradigms. Importantly, these cost advantages arise not solely from sequencing costs, but also from consolidating multiple diagnostic assays into a single, unified test and reducing the prolonged diagnostic odyssey. While SR-WGS represents an alternative first-tier approach that may offer lower upfront sequencing costs than LR-WGS, SR-WGS has reduced sensitivity for several variant classes highly relevant to hypotonia-associated diseases, including complex structural variants and methylation abnormalities. A direct cost-effectiveness comparison between SR-WGS and LR-WGS approaches is beyond the scope of this study. Therefore, future evaluations will be important for defining the optimal balance among cost, diagnostic yield, and clinical utility. It should be noted that our cost analysis focused on costs and does not take into account many indirect costs associated with the traditional testing paradigm, including the economic burden described above, associated with delayed or absent diagnoses for many patients. The analysis also does not consider the cost savings associated with a simplified consolidated laboratory workflow utilizing a single LRS assay compared to traditional multi-testing platforms. Additionally, cost estimates for the LRS-based hypotonia panel were derived from institutional cost-of-production data and may vary across settings.

This study demonstrates the diagnostic potential of LR-WGS in patients with hypotonia; however, several limitations of our current workflow should be acknowledged. First, the analysis was restricted to known genes and loci associated with hypotonia, with a primary focus on coding regions. This constraint may have limited the detection of pathogenic structural variants (SVs) and copy number variants (CNVs) in novel genes or non-coding regulatory regions, which may exert positional or regulatory effects on gene function. Similarly, methylation profiling in this study was limited to predefined disease-associated loci rather than encompassing a genome-wide analysis. Unlike short-read sequencing, there are currently no standards or guidelines on best practices for secondary and tertiary analysis of LR-WGS data. This, along with the lack of control and disease datasets to annotate frequencies of novel SVs, limits the scaling of LR-WGS in clinical laboratories. However, our approach here circumvents some of those limitations by focusing the analysis on hypotonia loci, reducing the burden of genome-wide variant interpretation.

Conclusion

This study demonstrates that LR-WGS with targeted analysis can serve as a single, cost-effective, unified diagnostic platform for the comprehensive detection of all genetic and epigenetic etiologies of hypotonia-associated diseases. In addition to consolidating different types of molecular assays into one workflow, which will likely shorten the diagnostic odyssey for many hypotonia patients and reduce associated health economic burdens, this diagnostic approach can successfully uncover missed diagnoses as well as novel genomic and epigenomic insights, which will strengthen our understanding of these diseases, eventually leading to more accurate management of patients with hypotonia.

Abbreviations

CMA	Chromosomal microarray analysis
CNVs	Copy number variants
CNS	Central nervous system
ddPCR	Droplet digital PCR
DM	Myotonic dystrophy
DM1	Myotonic dystrophy type 1
DM2	Myotonic dystrophy type 2
DMD	Duchenne muscular dystrophy
FXS	Fragile X syndrome
HGMD	Human Gene Mutation Database
IGV	Integrated Genomics Viewer
Indels	Insertions and deletions
LR-WGS	Long-read whole-genome sequencing
LRS	Long-read sequencing
MD	Muscular dystrophy
MS-MLPA	Methylation-specific multiplex ligation-dependent probe amplification
MS-PCR	Methylation-specific PCR
OMIM	Online Mendelian Inheritance in Man
PWS/AS	Prader–Willi syndrome/Angelman syndrome
SNVs	Single-nucleotide variants
SMA	Spinal muscular atrophy
SRS	Short-read sequencing
STRs	Short tandem repeats

TP-PCR	Triplet repeat-primed PCR
WES	Whole-exome sequencing
WGS	Whole-genome sequencing
5′UTR	5′ Untranslated region

Supplementary Information

The online version contains supplementary material available at https://doi.org/10.1186/s12916-026-04850-8.

Additional file 1. Supplementary Methods. Detailed description of the sequencing workflow, including library preparation and sequencing protocols, basecalling and read processing, variant calling, filtering and prioritization of pathogenic structural variantsand copy number variants, filtering and prioritization of small nucleotide variants, and PCR validation.

Additional file 2. Table S1-S8. Table S1: List of all patients along with gender, age, testing type, cost, diagnostic duration, and outcome. Table S2: Summary statistics of cohort characteristics, testing strategies, and diagnostic yield. Table S3: Summary statistics of diagnostic yield by testing strategy. Table S4: Overview and summary statistics of samples in Undiagnosed and Positive Reference Group for long read sequencing. Table S5: List of genes associated with hypotonia. Inheritance of geneas categorised by HGMD, OMIMand The Gene Curation Coalition. Table S6: Number of genomic variants detected in negative cohort - CNVs, SVs, and SNVs. Table S7: Validated pathogenic variants detected in the undiagnosed group; assays and the PCR primers used for validation. Table S8: Total testingcosts in all cohort and in patients receiving single or multiple testing.

Additional file 3. Supplementary Figures S1-S2. Supplementary Fig. S1: SNV/indel calls validation. Supplementary Fig. S2: Methylation profiling of PWS, Fragile X, and SMA regions in the undiagnosed cohort.

Additional file 4. Uncropped gel image for PCR validation.

Acknowledgements
We would like to thank members of the Dubai Health Genomics Medicine Center for their support and assistance in this study.

Authors' contributions
E.A. and A.AT. drafted the initial version of the manuscript. E.A., M.E.N., and R.J. generated and analyzed genomic data in the retrospective cohort. E.A. F.R., and I.C. performed the long read sequencing. E.A. prepared figures 1, 2, 4a, 5c, 6 and all supplementary Tables 1-8. S.S. and S.R. performed bioinformatics analysis of long-read sequencing data. S.S. prepared figure 3, 4, 5 and supplementary figures 1-2. A.A.T. conceived the project, secured funding, and supervised the work. S.K, R.S, O.A, F.A, A.A.A contributed to manuscript revision. All authors read and approved the final manuscript.

Funding
This study received institutional funding from Al Jalila Foundation and Mohammed Bin Rashid University (Dubai Health).

Data availability
All aggregated and summary-level data underlying the findings of this study, including information on the types of clinical tests performed, associated costs, patient numbers, and sequencing statistics for samples from the Undiagnosed Group and the Positive Reference Group, are provided in the Additional file 2: Table S1-S8. Access to raw data for the long-read sequenced samples is not publicly available under the UAE Federal Law by Decree No. (49) of 2023 "Regulating the Use of the Human Genome" to preserve individuals' privacy.

Declarations

Ethics approval and consent to participate
All patients or the legal guardians of pediatric participants consented to clinical genetic testing under a de-identified research protocol which was reviewed and approved by the Dubai Scientific Research Ethics Committee, Dubai Health Authority (approvals no. DSREC-SR-05/2024_03 and DSREC-08/2024_09).

Consent for publication
Not applicable.

Competing interests
The authors declare no competing interests.

Author details
[1]Mohammed Bin Rashid University of Medicine and Health Sciences, Dubai Health, Dubai, UAE. [2]Dubai Health Genomic Medicine Center, Dubai Health, Dubai, UAE. [3]Center for Genomic Discovery, Mohammed Bin Rashid University of Medicine and Health Sciences, Dubai Health, Dubai, UAE. [4]Dubai Health Authority, Dubai, UAE.

Received: 14 December 2025 Accepted: 31 March 2026
Published online: 08 April 2026

References

1. Bodensteiner JB. The evaluation of the hypotonic infant. Semin Pediatr Neurol. 2008;15:10–20.
2. Sparks SE. Neonatal hypotonia. Clin Perinatol. 2015;42:363–71. https://doi.org/10.1016/j.clp.2015.02.008.
3. K V MA, Mao R, Toth JN, Fulmer ML, Egense AS, Shankar SP. Prader-Willi and Angelman Syndromes: Mechanisms and management. Ther Clin Risk Manag. 2023;16:41–52. https://doi.org/10.2147/TACG.S372708
4. Quartier A, Poquet H, Gilbert-Dussardier B, Rossi M, Casteleyn AS, Portes VD, et al. Intragenic FMR1 disease-causing variants: a significant mutational mechanism leading to Fragile-X syndrome. Eur J Hum Genet. 2017;25:423–31. https://doi.org/10.1038/ejhg.2016.204.
5. Lisi EC, Cohn RD. Genetic evaluation of the pediatric patient with hypotonia: perspective from a hypotonia specialty clinic and review of the literature. Dev Med Child Neurol. 2011;53:586–99. https://doi.org/10.1111/j.1469-8749.2011.03918.x.
6. Morton SU, Christodoulou J, Costain G, Muntoni F, Wakeling E, Wojcik MH, et al. Multicenter consensus approach to evaluation of neonatal hypotonia in the genomic era: a review. JAMA Neurol. 2022;79:405. https://doi.org/10.1001/jamaneurol.2022.0067.
7. Pappalardo A, Pitto L, Fiorillo C, Donati MA, Bruno C, Santorelli FM. Neuromuscular disorders in Zebrafish: state of the art and future perspectives. NeuroMol Med. 2013;15:405–19. https://doi.org/10.1007/s12017-013-8228-z.
8. Rathore G, Kang PB. Pediatric neuromuscular diseases. Pediatr Neurol. 2023;149:1–14. https://doi.org/10.1016/j.pediatrneurol.2023.08.034.
9. Gonzalez-Quereda L, Rodriguez MJ, Diaz-Manera J, Alonso-Perez J, Gallardo E, Nascimento A, et al. Targeted next-generation sequencing in a large cohort of genetically undiagnosed patients with neuromuscular disorders in Spain. Genes. 2020;11:539. https://doi.org/10.3390/genes11050539.
10. Benarroch L, Bonne G, Rivier F, Hamroun D. The 2024 version of the gene table of neuromuscular disorders (nuclear genome). Neuromuscul Disord. 2023;34:126–70. https://doi.org/10.1016/j.nmd.2023.12.007.
11. Fardeau M, Desguerre I. Diagnostic workup for neuromuscular diseases. In: Dulac O, Lassonde M, Sarnat HB, editors. Handbook of Clinical Neurology. Amsterdam: Elsevier; 2013;1291–7. https://doi.org/10.1016/b978-0-444-59565-2.00001-0
12. Sullivan JA, Schoch K, Spillmann RC, Shashi V. Exome/genome sequencing in undiagnosed syndromes. Annu Rev Med. 2023;74:489–502. https://doi.org/10.1146/annurev-med-042921-110721.
13. Thornton CA. Myotonic dystrophy. Neurol Clin. 2014;32:705–19. https://doi.org/10.1016/j.ncl.2014.04.011.
14. Hagerman RJ, Berry-Kravis E, Hazlett HC, Bailey DB, Moine H, Kooy RF, et al. Fragile X syndrome. Nat Rev Dis Primers. 2017;3(1):17065. https://doi.org/10.1038/nrdp.2017.65.
15. Ciobanu CG, Nucă I, Popescu R, Antoci LM, Caba L, Ivanov AV, et al. Narrative review: update on the molecular diagnosis of Fragile X syndrome. Int J Mol Sci. 2023;24:9206. https://doi.org/10.3390/ijms24119206.

16. Rabea F, Naofal ME, Chekroun I, Khalaf M, Zaabi NA, AlZaabi K, et al. Spinal muscular atrophy genetic epidemiology and the case for premarital genomic screening in Arab populations. Commun Med. 2024;4:119. https://doi.org/10.1038/s43856-024-00548-1.
17. Negi S, Stenton SL, Berger SI, Canigiula P, McNulty B, Violich I, et al. Advancing long-read nanopore genome assembly and accurate variant calling for rare disease detection. Am J Hum Genet. 2025;112:428–49. https://doi.org/10.1016/j.ajhg.2025.01.002.
18. Yu SY, Xi YL, Xu FQ, Zhang J, Liu YS. Application of long-read sequencing in rare diseases: the longer, the better? Eur J Med Genet. 2023;66:104871. https://doi.org/10.1016/j.ejmg.2023.104871.
19. Naofal ME, Ramaswamy S, Alsarhan A, Nugud A, Sarfraz F, Janbaz H, et al. The genomic landscape of rare disorders in the Middle East. Genome Med. 2023;15:5. https://doi.org/10.1186/s13073-023-01157-8.
20. Richards S, Aziz N, Bale S, Bick D, Das S, Gastier-Foster J, et al. Standards and guidelines for the interpretation of sequence variants: a joint consensus recommendation of the American College of Medical Genetics and Genomics and the Association for Molecular Pathology. Genet Med. 2015;17:405–24. https://doi.org/10.1038/gim.2015.30.
21. EPI2ME Labs. wf-human-variation: Human variation workflow, version 2.6.0. Oxford: Oxford Nanopore Technologies; 2024.
22. Sedlazeck FJ, Rescheneder P, Smolka M, Fang H, Nattestad M, Von Haeseler A, et al. Accurate detection of complex structural variations using single-molecule sequencing. Nat Methods. 2018;15:461–8. https://doi.org/10.1038/s41592-018-0001-7.
23. Jiang T, Liu Y, Jiang Y, Li J, Gao Y, Cui Z, et al. Long-read-based human genomic structural variation detection with cuteSV. Genome Biol. 2020;21(1):189. https://doi.org/10.1186/s13059-020-02107-y.
24. Amberger JS, Bocchini CA, Schiettecatte F, Scott AF, Hamosh A. OMIM.org: online mendelian inheritance in man (OMIM®), an online catalog of human genes and genetic disorders. Nucleic Acids Res. 2014;43:D789-98. https://doi.org/10.1093/nar/gku1205.
25. DiStefano MT, Goehringer S, Babb L, Alkuraya FS, Amberger J, Amin M, et al. The gene curation coalition: a global effort to harmonize gene–disease evidence resources. Genet Med. 2022;24:1732–42. https://doi.org/10.1016/j.gim.2022.04.017.
26. Mercuri E, Bönnemann CG, Muntoni F. Muscular dystrophies. Lancet. 2019;394:2025–38. https://doi.org/10.1016/s0140-6736(19)32910-1.
27. Landrum MJ, Lee JM, Benson M, Brown GR, Chao C, Chitipiralla S, et al. ClinVar: improving access to variant interpretations and supporting evidence. Nucleic Acids Res. 2017;46:D1062-7. https://doi.org/10.1093/nar/gkx1153.
28. Rehm HL, Berg JS, Brooks LD, Bustamante CD, Evans JP, Landrum MJ, et al. ClinGen: the Clinical Genome Resource. N Engl J Med. 2015;372:2235–42. https://doi.org/10.1056/nejmsr1406261.
29. Henkhaus RS, Kim SJ, Kimonis VE, Gold JA, Dykens EM, Driscoll DJ, et al. Methylation-specific multiplex ligation-dependent probe amplification and identification of deletion genetic subtypes in Prader-Willi syndrome. Genet Test Mol Biomarkers. 2011;16:178–86. https://doi.org/10.1089/gtmb.2011.0115.
30. Sinha S, Rabea F, Ramaswamy S, Chekroun I, Naofal ME, Jain R, et al. Long-read sequencing enhances pathogenic and novel variation discovery in patients with rare diseases. Nat Commun. 2025;16:2500. https://doi.org/10.1038/s41467-025-57695-9.
31. De Boer EN, Scheper AJ, Hendriksen D, Charbon B, van der Vries G, Berge AMT, et al. Nanopore long-read sequencing as a first-tier diagnostic test to detect repeat expansions in neurological disorders. Int J Mol Sci. 2025;26:2850. https://doi.org/10.3390/ijms26072850.
32. EveryLife Foundation for Rare Diseases. The cost of delayed diagnosis in rare disease: a health economic study. Silver Spring (MD): EveryLife Foundation for Rare Diseases; 2023.
33. Briñas L, Richard P, Quijano-Roy S, Gartioux C, Ledeuil C, Lacène E, et al. Early onset collagen VI myopathies: genetic and clinical correlations. Ann Neurol. 2010;68:511–20. https://doi.org/10.1002/ana.22087.
34. Bönnemann CG. The collagen VI-related myopathies. In: Dulac O, Lassonde M, Sarnat HB, editors. Handbook of Clinical Neurology. Amsterdam: Elsevier; 2011. p. 81–96.
35. Butterfield RJ, Foley AR, Dastgir J, Asman S, Dunn DM, Zou Y, et al. Position of glycine substitutions in the triple helix of COL6A1, COL6A2, and COL6A3 is correlated with severity and mode of inheritance in collagen VI myopathies. Hum Mutat. 2013;34(11):1558–67. https://doi.org/10.1002/humu.22429.
36. ClinVar. Variation ID 449325. Bethesda (MD): National Center for Biotechnology Information (NCBI); 2025. https://www.ncbi.nlm.nih.gov/clinvar/variation/449325/.
37. ClinVar. Variation ID 581383. Bethesda (MD): National Center for Biotechnology Information (NCBI); 2025. https://www.ncbi.nlm.nih.gov/clinvar/variation/581383/.
38. Nobile V, Pucci C, Chiurazzi P, Neri G, Tabolacci E. DNA methylation, mechanisms of FMR1 inactivation and therapeutic perspectives for fragile X syndrome. Biomolecules. 2021;11(2):296. https://doi.org/10.3390/biom11020296.
39. Driscoll DJ, Miller JL, Cassidy SB. Prader-Willi syndrome. In: Adam MP, Everman DB, Mirzaa GM, et al., editors. GeneReviews®. Seattle (WA): University of Washington, Seattle; 1993–2024. https://www.ncbi.nlm.nih.gov/books/NBK1
40. Marakhonov AV, Tabakov V, Zernov NV, Dadali EL, Sharkova IV, Skoblov M. Two novel COL6A3 mutations disrupt extracellular matrix formation and lead to myopathy from Ullrich congenital muscular dystrophy and Bethlem myopathy spectrum. Gene. 2018;672:165–71. https://doi.org/10.1016/j.gene.2018.06.026.
41. Ozisik O, Gorokhova S, Cerino M, Bartoli M, Baudot A. System-level analysis of genes mutated in muscular dystrophies reveals a functional pattern associated with muscle weakness distribution. Sci Rep. 2024;14(1):11225. https://doi.org/10.1038/s41598-024-60761-9.
42. Kachuei M, Orangi K, Mohammadi A, Mohammadi M, Mojbafan M. Bethlem myopathy: a novel homozygous variant of c.385C>T (p.Arg129Cys) in the COL6A2 gene. Clin Case Rep. 2024;12(8):e9306. https://doi.org/10.1002/ccr3.9306.

Publisher's Note